IMPROVED PERFORMANCE OF LARGE STROKE COMB-DRIVE ACTUATORS BY USING A STEPPED FINGER SHAPE

J.B.C. Engelen[1], M.A. Lantz[2], H.E. Rothuizen[2], L. Abelmann[1], and M.C. Elwenspoek[1,3]*
[1] MESA+ and IMPACT Research Institutes, University of Twente, Enschede, The Netherlands
[2] IBM Research, Zürich Research Laboratory, Rüschlikon, Switzerland
[3] Freiburg Institute for Advanced Studies (FRIAS), Albert-Ludwigs-Universität, Freiburg, Germany

ABSTRACT

In this work we describe an electrostatic mass-balanced planar *x*/*y*-scanner, using an optimized comb finger shape, designed for parallel-probe storage applications. We show a new stepped comb finger shape design, that has superior force/displacement characteristics leading to a larger stroke at the same voltage and a larger available force compared to straight or tapered shapes.

KEYWORDS

Probe storage, MEMS, DRIE, comb drive, electrostatic actuator, finite-element analysis (FEA)

INTRODUCTION

One of the promising candidates for future storage applications is parallel-probe data storage, in which many atomic-force-microscope-like probes are operated in parallel to read and write data at a high data rate and a high data density (> 1 Tb/in^2) [1, 2]. Below the array of probes, the storage medium is moved in *x* and *y* directions by a positioning system (the scanner) with nanometer accuracy. To fully utilize the storage medium, the scanner's displacement range should be larger than the distance between the probes. As the probe density is on the order of 100 cantilevers/mm^2 [3], the scan range has to be relatively large, on the order of ± 50 µm.

Shock resistance and low power consumption are important requirements for mobile probe-storage applications [4]. Previously, a shock-resistant scanner design using electromagnetic actuation was reported by Lantz *et al.* [4]. Here we explore electrostatic actuation with shaped comb drive fingers as an alternative to the electromagnetic actuation used in [4], because, in principle, comb drives do not require power to maintain a non-equilibrium position. Thus during track follow, when one axis is stationary and the other is moving slowly, the power consumption of comb drives is potentially lower compared to electromagnetic actuation.

DESIGN

In order to achieve shock resistance in the planar *x* and *y* directions while being compliant for actuation, we adopt the mass-balancing concept from [4]. To move the scan table 50 µm in both positive and negative *x* and *y* directions, four comb drives, consisting of a fixed stator and a moving translator, are used (see Figure 1). The comb drives are coupled to the scan table through pivoting elements, such that the scan table and translator move in opposite directions. When the scan table and translator masses are matched, the system is mass-balanced for enhanced linear shock resistance. A large out-of-plane stiffness for passive shock rejection in the *z* direction is achieved by etching the device, including the spring suspension, through the full thickness of the wafer (400 µm). This large etch depth necessitates the use of a relatively large gap between fingers (25 µm), resulting in a reduced actuation force. To increase the generated force without decreasing the minimum etch trench width, two comb finger shapes are investigated: a tapered shape [5, 6] and a new 'stepped' shape, both shown in Figure 2.

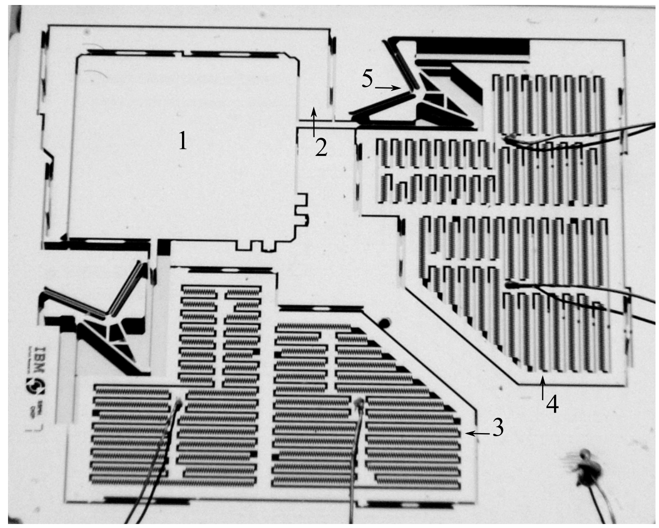

Figure 1: Photograph of a fabricated device (2x2 cm). 1: scan table, 2: C-bracket, 3: x comb drives, 4: y comb drives, 5: pivoting element. The wires are electrical connections to the isolated stators and to ground the moving parts of the device (bottom right).

To perform seek operations or compensate for residual shock forces, the actuation force at any given position *x* must exceed the suspension spring restoring force. The force available for these control operations is

$$F_{\text{avail}}(x) = F_{\text{comb}}(x, V_{\max}) - kx, \quad (1)$$

$$F_{\text{avail}}(x) = \frac{1}{2} N \frac{\partial C}{\partial x} V_{\max}^2 - kx, \quad (2)$$

where F_{comb} is the actuation force generated by the comb drive, V_{max} the maximum available voltage, k the spring constant of the suspension, x the displacement, N the number of finger pairs, and C the capacitance of one finger pair. This available force F_{avail} should be greater than zero within the operating range to enable control operations and ideally should be as large as possible. Figure 3 shows a simulation result for the available force curve for a normal straight finger shape, from which it can be seen that the force available at large positive displacements needs to be increased in order to extend the range of achievable displacement and to provide a positive force margin for control operations.

The available force curve can be tailored by increasing the number of finger pairs N, by reducing the spring stiffness k, by modifying the individual comb finger lengths [7], or by changing the comb finger shape [8]. Increasing the number of finger pairs increases the footprint and mass of the scanner and is therefore unattractive. Because a minimum out-of-plane stiffness is required, reduction of k is limited; we use the same stiffness as in [4] for easier direct comparison. Modifying individual finger lengths decreases the force at small displacements and does not increase the force for large displacements. Conversely, 'gap-narrowing' finger shapes (i.e. shapes that narrow the gap between fingers at larger displacements) increase the force for large displacements and is therefore most suited for our application. For straight fingers, the necessary change in capacitance $\frac{\partial C}{\partial x}$ is caused by increasing finger overlap; for gap-narrowing finger shapes, an extra term due to the decreasing gap distance between fingers adds to the capacitance change, hence an increase in force. The gap-narrowing effect of the tapered and stepped shapes can be seen in Figure 2, when comparing the geometries at 0 and 50 µm displacement.

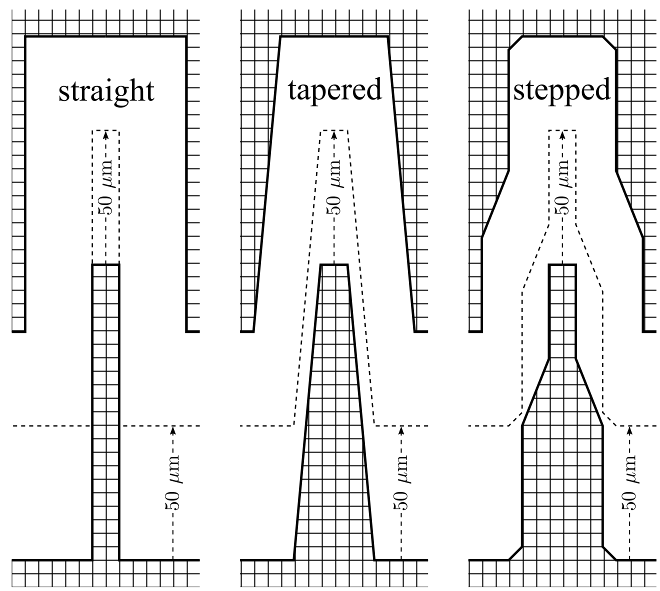

Figure 2: The three investigated finger shapes, showing the new stepped finger shape on the right. The dashed outline shows the geometry at 50 µm displacement.

FABRICATION

The scanner is fabricated from a 400 µm thick, highly-doped single-crystal silicon wafer, using deep reactive-ion etching and a layer of aluminum as an etch stop. All the mechanical parts including the comb drives are etched through the full thickness of the wafer. This is done to achieve high aspect ratio springs with a large out-of-plane stiffness for a large passive out-of-plane shock rejection [4]. The minimum trench width is 25 µm after etching, which is used as a constraint on the gap between fingers during the design of the finger shapes. A larger minimum width constraint of 40 µm is used at the base of the fingers (where the etch area is enclosed on 3 sides, instead of 2 sides for a continuous trench), to obtain a more homogeneous etch rate across the geometry. Larger openings are defined by a 25 µm trench following their periphery, leaving a center piece that drops out when the aluminum etch stop layer is removed.

The comb drive stators are completely surrounded by the translators; several break-out pieces connect the stators mechanically to the translators to prevent the stators from falling out at the end of the etch process. After etching, individual scanner chips are separated from the wafer and glued to base plates. A base plate features several arrays of supports on which glue is applied; the clearance between moving parts and base plate is about 100 µm. Then the break-out pieces are removed to provide electrical isolation between the stator and the translator of the comb drives. Finally, small wires are connected to the device using conducting epoxy.

RESULTS

Figure 3 shows 2D electrostatic finite-element results for the available force of the three finger shapes. Figure 4 shows the displacement versus voltage curve measurements for the tapered and stepped finger shape devices. The measured resonance frequencies for the corresponding axes of the tapered and stepped designs were 133 Hz and 147 Hz, respectively. Using these frequencies and measured actuator and scan table masses, finite-element simulations predict effective spring constants of 60 N/m and 72 N/m, respectively, although the suspensions should have identical stiffness by design. The difference stems from variations in the etch profiles actually obtained. At 120 V, displacements of 38 µm and 48 µm were measured for the tapered and stepped fingers, respectively (Figure 4), corresponding to 2.3 mN and 3.5 mN, respectively, using the calculated stiffness values. The equilibrium voltage V_{eq} measurements in Figure 4 are used to calculate the available force; combining equation (2)

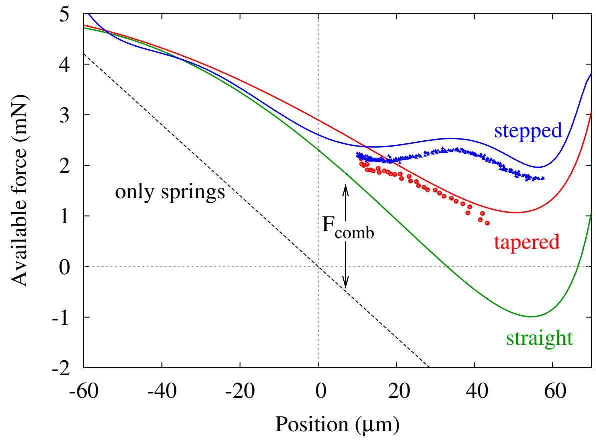

Figure 3: The maximum available force ($= F_{comb} - kx$) in the positive direction as calculated by 2D electrostatic FE simulations (solid lines, polynomial fit, V_{max} = 150 V; k = 72 N/m; 731 finger pairs) and as calculated from the measurements in Figure 4 (points). The dashed curve shows the force from the suspension springs only.

and the equilibrium condition

$$\frac{1}{2}N\frac{\partial C}{\partial x}V_{\text{eq}}^2 = kx, \tag{3}$$

we obtain

$$F_{\text{avail}}(x) = kx\frac{V_{\text{max}}^2}{V_{\text{eq}}^2} - kx. \tag{4}$$

The calculation results are shown as points in Figure 3; the difference with the finite-element result is explained by a slightly larger obtained finger gap size.

The device using stepped fingers reaches a 25% larger displacement than the device using tapered fingers, in spite of the 20% stiffer spring suspension of the stepped shape device. Stepped fingers provide the highest force and their available force curve is almost flat for positive displacements, approximating an optimal solution where the minimum in the available force curve is as high as possible. Assuming a maximum voltage of 150 V, the device using the stepped shape has at least 1.8 mN force available for control operations for the full ±50 µm range.

Interestingly, the available force is largest in the region where the fingers are disengaged and have no overlap ($x < -25$ µm); the comb drive force decreases, but the spring force increases and because the displacement is negative, it adds to the available force in the positive direction. Contrary to what one might expect, the minimum of the available force curve lies not in the region where the fingers are disengaged and F_{comb} is small, but in the region where F_{comb} is large and where the comb drive is close to instability (snap-in).

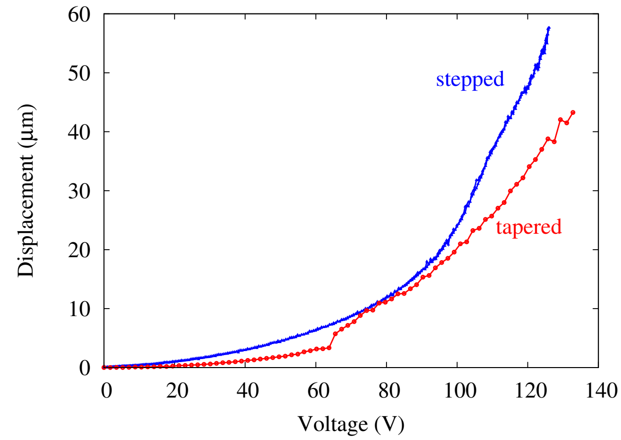

Figure 4: Displacement measurements on a device with tapered and a device with stepped fingers. The feature in the tapered finger curve at 65 V is a measurement error caused by video processing.

CONCLUSION

We have designed and successfully fabricated a mass-balanced vibration resistant *x*/*y*-scanner that uses electrostatic actuation. To provide passive shock rejection in the *z* direction perpendicular to movement, the *x*/*y*-scanner is fabricated from the full thickness of the wafer (400 µm). In order to etch comb drives through this thickness, the gap between comb drive fingers was relatively large (25 µm).

An important conclusion from the available force calculations is that, although the fingers are disengaged for large negative displacements, the available force in the positive direction is still large in this region due to the restoring spring force; the minimum available force in the positive direction is found at large positive displacements. This means that, in terms of available force, it is not necessary to have comb fingers overlap throughout the whole actuation range.

The comb drive force was increased by using gap-narrowing finger shapes. Measurements showed that the displacement at 120 V using stepped fingers is 26% more than using tapered fingers, despite the spring suspension of the stepped shape device being 20% stiffer than the spring stiffness of the device with tapered fingers. Moreover, the available force for control operations is larger for the stepped shape compared to the straight and tapered finger shapes. The available force curve of the stepped shape approximates an optimal solution where the available force curve is flat and its minimum is as high as possible.

ACKNOWLEDGEMENTS

We would like to thank Ute Drechsler for etching the structures, Richard Stutz for his help in drawing the structures, and Remco Sanders for his help with the displacement measurements. This research was supported financially by Technology Foundation STW.

REFERENCES

[1] R. J. Cannara, B. Gotsmann, A. Knoll, and U. Dürig, "Thermo-mechanical probe storage at Mbps single-probe data rates and Tbit in^2 densities," *Nanotechnol.*, vol. 19, p. 395305, 2008.

[2] A. Pantazi *et al.*, "Probe-based ultrahigh-density storage technology," *IBM J. Res. Dev.*, vol. 52, pp. 493–511, 2008.

[3] M. Despont, U. Drechsler, R. Yu, H. Pogge, and P. Vettiger, "Wafer-scale microdevice transfer/interconnect: Its application in an AFM-based data-storage system," *J. Microelectromech. Syst.*, vol. 13, pp. 895–901, 2004.

[4] M. A. Lantz, H. E. Rothuizen, U. Drechsler, W. Häberle, and M. Despont, "A vibration resistant nanopositioner for mobile parallel-probe storage applications," *J. Microelectromech. Syst.*, vol. 16, pp. 130–139, 2007.

[5] M. A. Rosa, S. Dimitrijev, and H. B. Harrison, "Enhanced electrostatic force generation capability of angled comb finger design used in electrostatic comb-drive actuators," *Electron. Lett.*, vol. 34, pp. 1787–1788, 1998.

[6] J. B. C. Engelen, H. E. Rothuizen, U. Drechsler, R. Stutz, M. Despont, L. Abelmann, and M. A. Lantz, "A mass-balanced through-wafer electrostatic *x*/*y*-scanner for probe data storage," *Microelectron. Eng.*, Article in Press, 2008, doi:10.1016/j.mee.2008.11.032.

[7] J. Grade, H. Jerman, and T. Kenny, "Design of large deflection electrostatic actuators," *J. Microelectromech. Syst.*, vol. 12, pp. 335–343, 2003.

[8] B. D. Jensen, S. Mutlu, S. Miller, K. Kurabayashi, and J. J. Allen, "Shaped comb fingers for tailored electromechanical restoring force," *J. Microelectromech. Syst.*, vol. 12, pp. 373–383, 2003.

CONTACT

* J.B.C. Engelen: j.b.c.engelen@utwente.nl